Low frequency acoustic stop bands in cubic arrays of thick spherical shells with holes

Guillaume Dupont
Aix Marseille Univ, CNRS, Centrale Marseille, IRPHE UMR 7342, 13013 Marseille, France

Alexander Movchan
Department of Mathematical Sciences, Liverpool University, Peach Street, Liverpool L69 3BX, UK

Stefan Enoch and Sébastien Guenneau
Aix Marseille Univ, CNRS, Centrale Marseille, Institut Fresnel UMR 7249, 13013 Marseille, France

We analyse the propagation of pressure waves within a fluid filled with a three-dimensional array of rigid coated spheres (shells). We first draw band diagrams for corresponding Floquet-Bloch waves. We then dig a channel terminated by a cavity within each rigid shell and observe the appearance of a low frequency stop band. The underlying mechanism is that each holey shell now acts as a Helmholtz resonator supporting a low frequency localized mode: Upon resonance, pressure waves propagate with fast oscillations in the thin water channel drilled in each shell and are localized in each fluid filled inner cavity. The array of fluid filled shells is approximated by a simple mechanical model of springs and masses allowing for asymptotic estimates of the low frequency stop band. We finally propose a realistic design of periodic macrocell with a large defect surrounded by 26 resonators connected by thin straight rigid wires, which supports a localized mode in the low frequency stop band.

I. INTRODUCTION: ACOUSTIC METAMATERIALS

In the tracks of photonic crystals, phononic crystals [1] have provided a fillip for research in acoustic stop band structures [2, 3] within which light or sound is prohibited to propagate due to multiple scattering between periodically spaced inclusions. In 2000, Liu *et al.* provided the first numerical and experimental evidence of locally resonant structures for elastic waves in 3D arrays of thin coated spheres [4] wherein low frequency stop bands occur. This seminal work paved the way towards acoustic analogues of electromagnetic meta-materials, such as fluid-solid composites [5]. Inspired by the research monograph on multi-structures [6], Movchan and Guenneau subsequently proposed to use arrays of cylinders with a split ring cross section as building blocks for 2D localised resonant acoustic structures displaying negative refraction [7, 8]. Such split ring resonators, introduced by John Pendry in the context of electromagnetic waves [9], also work for in-plane elastic waves [10]. Milton, Briane and Willis provided a thorough mathematical frame for such effects including cloaking for certain types of elastodynamic waves in structural mechanics [11]. For instance, coupled in-plane pressure and shear waves were numerically shown to be detoured around a finite size obstacle by a specially designed cloak with an anisotropic heterogeneous elasticity tensor (without the minor symmetries) [12]. Acoustic metamaterials via geometric transform can thus in theory achieve unprecented control of elastic and pressure waves [13, 14].

Li and Chan independently proposed a similar type of negative acoustic metamaterial [15]. In a recent work, Fang *et al.* experimentally demonstrated a dynamic effective negative stiffness in a chain of water filled Helmholtz's resonators for ultrasonic waves [16]. It has been also shown using homogenisation theory that surface water waves propagating within an array of fluid filled Helmholtz's resonators display a negative effective density [17]. A focussing effect through a finite array of such resonators was numerically achieved, with a resolution of a third of the wavelength. Similar effects have been experimentally demonstrated for a doubly periodic array of Helmholtz's resonators shaped as soda cans [18]. In the present paper, we would like to extend these concepts to pressure waves propagating in a three-dimensional array of resonators.

II. MOTIVATION: SPECTRAL PROPERTIES OF A PERIODIC ARRAY OF RIGID SPHERES

As a preamble, let us start with an illustrative numerical result for a spectral problem for the Helmholtz operator within a periodic cubic array of rigid spheres: the unknown is a pressure wave field, here sound in water (wave speed $c = 1483\ m.s^{-1}$). Neumann boundary conditions are prescribed on the contour of each defect and standard Floquet-Bloch conditions are set on an elementary cell of the periodic structure. The finite element formulation was implemented in the COMSOL Multiphysics Package to compute the eigenvalues and to generate the corresponding eigenfields. We present in figure 1 the structure and in figure 2 the corresponding dispersion diagram for eigenfrequencies ω as a function of the Floquet-Bloch parameter k: along the horizontal axis we have the values of modulus of $\mathbf{k}$, where k stands for the position vector of a point on the contour ΓXMU within the irreducible Brillouin zone. We note the absence of bandgaps with the presence of rigid spheres. This lack of intervals of forbidden frequencies motivates the present study: how can one create a stop band without further increasing the

size of the rigid spheres?

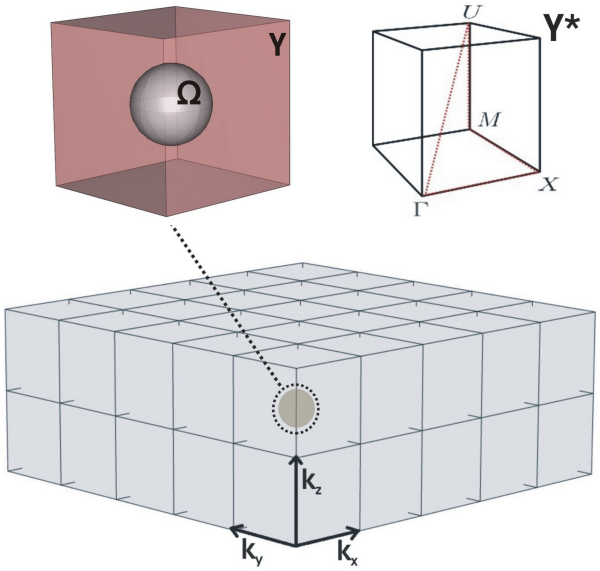

FIG. 1: Three-dimensionnal phononic crystal, periodic cell Y with a rigid sphere Ω in physical space and and irreducible Brillouin zone ΓXMU of the periodic cell Y^* in reciprocal space with the three components of the Floquet-Bloch vector $\mathbf{k} = (k_x, k_y, k_z)$.

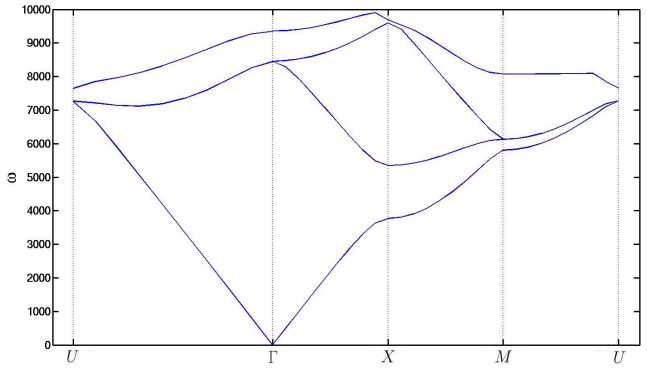

FIG. 2: Dispersion diagram for a periodic array (pitch $d =$ 1m) of spherical rigid inclusions ($R = 0.4$m) representing the frequency ω (Hz) of pressure waves in water, versus the wavenumber $|\mathbf{k}|$ (m^{-1}), projection of the Bloch vector $\mathbf{k}$ along the edges of ΓXMU.

III. SETUP OF THE SPECTRAL PROBLEM: THE CONTINUUM MODEL

Let us first recall the finite element set-up. Let $u(x, y, z)$ satisfy the Helmholtz equation:

$$\nabla.\left(\frac{1}{\rho(x,y,z)}\nabla u(x,y,z)\right) + \frac{\omega^2}{\lambda(x,y,z)}u(x,y,z) = 0 \quad (1)$$

where ρ, λ and u are the density, the bulk modulus and the pressure field.

Due to the periodicity of the lattice, it is customary to require that the eigenfunctions be of the Floquet-Bloch type. So, for a cubic array of unit cells Y,

$$u(x+1, y+1, z+1) = u(x, y, z)e^{i(k_x+k_y+k_z)} \quad (2)$$

where k_x, k_y and k_z are components of the Bloch vector $\mathbf{k}$ within the Brillouin zone $Y^* = [0, \pi]^3$.

The implementation in the finite element package is fairly straightforward. We first multiply equation (1) by a smooth function V and using the Green's formula, we obtain the so-called weak form of the time-harmonic acoutic equation

$$-\int_Y \rho^{-1}\nabla u.\nabla V dxdydz + \int_{\partial Y} \rho^{-1}\left(\frac{\partial u}{\partial n}V - \frac{\partial V}{\partial n}u\right)ds + \omega^2 \int_Y \lambda^{-1} uV dxdydz = 0 \quad (3)$$

where $\partial f/\partial n = \nabla f \cdot \mathbf{n}$ with $\mathbf{n}$ the unit outward normal to the boundary ∂Y of Y, and ds the infinitesimal surface element on ∂Y.
We note that the weak formulation holds for heterogeneous fluids as ρ and λ can be spatially varying. In particular, this model works for perforated domains such as a homogeneous fluid filled with a periodic array of rigid osbtacles. For the finite element implementation, (3) is discretised using test functions taking values on nodes of a tetrahedral mesh of the basic cell (first order tetrahedral elements), see e.g. [19] for further details. From (3), we note that setting rigid boundary conditions conditions on an inclusion amounts to assuming Neumann (natural) homogeneous data, whereas transmission conditions at the interface between various fluid phases mean that the quantity $\rho^{-1}\partial u/\partial n$ is preserved across the interface.
Let us now consider a periodic array of defects $\Omega_1, ..., \Omega_N$ embedded in an elementary cell $Y =]0; 1[^3$. Let $u(x, y, z)$ satisfy the Helmholtz equation in $Y \setminus \bigcup_{j=1}^N \overline{\Omega_j}$. We also assume that u satisfies Neumann boundary condiditons on the contours of defects, where $\mathbf{n}$ denotes the unit outward normal to the boundary $\partial\Omega_j$ of a defect Ω_j:

$$\left.\frac{\partial u}{\partial n}\right|_{\partial\Omega_j} = 0\,, \quad j = 1, ..., N \quad (4)$$

We would like to consider a particular case when the defects $\Omega_1, ..., \Omega_N$ are spherical shells with thin water channels connecting a fluid-filled interior cavity to the exterior surrounding fluid. These defects can be modelled as multistructures [6] in the following way,

$$\Omega_{(N)} = \left\{a_{(N)} < \sqrt{x^2+y^2+z^2} < b_{(N)}\right\} \setminus \overline{\bigcup_{j=1}^N \Pi^{(j)}_{\varepsilon(N)}} \quad (5)$$

where $a_{(N)}$ and $b_{(N)}$ are given constants and $\Pi^{(j)}_{\varepsilon(N)}$ is the thin channel.

IV. ASYMPTOTIC APPROXIMATION: A DISCRETE SPRING-MASS MODEL

In this section, we derive an asymptotic approximation of the field within thin channels $\Pi^{(j)}_\varepsilon$,

$$\Pi^{(j)}_\varepsilon = \{(x,y,z) \,:\, 0<x<l_j, \\ \sqrt{y(t)^2+z(t)^2} < \varepsilon h_j(t),\, (0\le t\le 2\pi)\Big\} \quad (6)$$

where l_j is the length of the j^{th} bridge, $\varepsilon h_j(t)$ the radius of its varying cross-section D_ε (parametrized by t). Here, ε is a small positive non-dimensionnal parameter. To derive the asymptotic expansions, we introduce the scaled variables $\xi = (y/\varepsilon, z/\varepsilon)$.

Without loss of generality, and for the sake of simplicity, we drop the superscript j. In Π_ε, the time-harmonic wave equation takes the rescaled form

$$\left\{\frac{1}{\rho}\left(\frac{1}{\varepsilon^2}\Delta_\xi + \frac{\partial^2}{\partial x^2}\right) + \frac{\omega^2}{\lambda}\right\} u = 0\,, \quad (7)$$

with the Neumann boundary conditions

$$\left.\frac{\partial u}{\partial n}\right|_{\partial D_\xi} = 0 \quad (8)$$

The field u is approximated in the form

$$u \sim u^{(0)}(x,y,z) + \varepsilon^2 u^{(1)}(x,y,z) \quad (9)$$

To leading order, we obtain

$$\left\{\begin{array}{rcll} \Delta_\xi u^{(0)} &=& 0 & \text{on} \quad D_\xi \\ \nabla_\xi u^{(0)} &=& 0 & \text{on} \quad \partial_{D_\xi} \end{array}\right. \quad (10)$$

Hence, $u^{(0)} = u^{(0)}(x)$ (it is $\xi,\zeta-$independent). Assuming that $u^{(0)}$ is given, we derive that the function $u^{(1)}$ satisfies the following model problem on the scaled cross-section of Π_ε

$$\left\{\begin{array}{rcll} \Delta_\xi u^{(1)} &=& -\dfrac{1}{\rho}\dfrac{\partial^2 u^{(0)}}{\partial x^2} + \dfrac{\omega^2}{\lambda}u^{(1)} & \text{in} \quad D_\xi \\ \nabla_\xi u^{(1)}\cdot \mathbf{n} &=& 0 & \text{on} \quad \partial_{D_\xi} \end{array}\right. \quad (11)$$

The condition of solvability for the problem has the form:

$$\frac{1}{\rho}\frac{d^2u^{(0)}}{dx^2} + \frac{\omega^2}{\lambda}u^{(0)} = 0\,, \quad 0<x<l_j \quad (12)$$

Hence, we have shown that to the leading order we can approximate the field u within the thin channel Π_ε by the function $u^{(0)}$ which satisfies the Helmholtz's equation in one-space dimension. We now assume that the field is periodic over the cell since it is localized. This shows that the average of the eigenfield over the macro-cell vanishes. Indeed, let χ_1 denotes the value of the field in the large body Σ of the multi-structure Ω and let χ_2 (which we normalize to 1) denotes the value of the field within the complementary area of the macro-cell $Y\setminus\Omega$ excluding the thin channels. Taking $V=1$ in (3), we deduce that

$$\omega^2\int_Y \rho u dxdydz = -\int_{\partial Y\cup\partial\Omega}\lambda\frac{\partial u}{\partial n}dS = 0 \quad (13)$$

This shows that the average of the field u over Y vanishes, hence by neglecting the volume of the thin channels, we obtain

$$\chi_1 meas_\Sigma + \chi_2 meas_{Y\setminus\Omega} = O(\varepsilon) \quad (14)$$

where $meas_\Sigma$ and $meas_{Y\setminus\Omega}$ denote respectively the areas of Σ and $Y\setminus\Omega$.

We now consider two cases. The first one is the study of an array of simple spherical shells with either one or six thin channels, and the other one is the study of an array of double spherical shells with one thin channel in each shell. Since we have p thin channels, we have p separate eigensolutions V_j, $(j=1,...,p)$, corresponding to the vibrations of thin domains $\Pi^{(j)}_\varepsilon$

$$\rho^{-1}V_j''(x) + \lambda^{-1}\omega^2 V_j(x) = 0\,, \quad 0<x<l_j\,, \quad (15)$$

$$V_j(0) = \chi_2 = -\chi_1\frac{meas(\Xi)}{meas(Y\setminus\Omega)}\,, \quad (16)$$

$$\lambda^{-1}I_j V_j'(l_j) = M_j\omega^2 V_j(l_j)\,, \quad (17)$$

where

$$I_j = \int_0^{2\pi}\varepsilon h_j(t)\,dt \quad (18)$$

All the channels are connected to Ξ, hence, $V_1(l_1) = ... = V_p(l_p) = V$. We note that $V_j(0)$ is equal to a non-zero constant.

The solution of the problem $(15)-(17)$ has the form

$$V_j(x) = -\frac{\chi_2[\cos((\omega/c)l_j)-1]}{\sin((\omega/c)l_j)}\sin\left(\frac{\omega}{c}x\right) + \chi_2\cos\left(\frac{\omega}{c}x\right) \quad (19)$$

where $c=\sqrt{\lambda/\rho}$ and the frequency ω is given as the solution of the following equation:

$$\sum_{j=1}^{n}\left(I_j \cot\left(\frac{\omega l_j}{c}\right)\right) = \frac{m_j c}{\lambda}\omega \qquad (20)$$

where we invoked Newton's second law. Looking at a first low frequency, we deduce an explicit asymptotic approximation

$$\omega \sim \sqrt{\sum_{j=1}^{n}\left(\frac{I_j}{l_j}\right)}\sqrt{\frac{\lambda}{M}}\left(1+\frac{meas(\Xi)}{meas(Y\setminus\Omega)}\right) \qquad (21)$$

This estimate actually holds for the frequency ω_2 of the upper edge of the phononic band gap. We note that if we take $V(0)=0$ instead of $V(0)=meas(\Xi)/meas(Y\setminus\Omega)$, we estimate the frequency of the lower-edge of the phononic band gap.

A. Eigenfrequency estimate in the case of a single spherical shell with one or six thin channels

We report in figures (4) and (7) finite element computations for a periodic cell of sidelength d with a simple spherical shell with thin channels. The interior and exterior radii of the shell are respectively 0.3m and 0.4m, the thin channels have the same length 0.1m and radii 0.01m. Therefore, the frequency estimates are (in Hertz):

$$\omega_1 \sim 227.301 \quad , \quad \omega_2 \sim 235.889 \qquad (22)$$

for one thin channel, which are in good agreement with the finite element values

$$\omega_1^* = 224.6155 \quad , \quad \omega_2^* = 241.3825 \qquad (23)$$

for one thin channel, and

$$\omega_1 \sim 556.772 \quad , \quad \omega_2 \sim 577.809 \qquad (24)$$

for six thin channels, which are in good agreement with the finite element values

$$\omega_1^* = 548.3515 \quad , \quad \omega_2^* = 588.8909 \qquad (25)$$

for six thin channels.
This demonstrates that the discrete model provides accurate estimates for the lower and upper edges of the ultra-low frequency stop band. This is therefore a useful tool which can be used in the design of acoustic metamaterials.

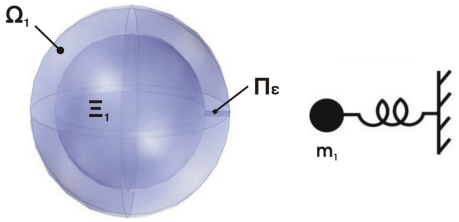

FIG. 3: Geometry of the inclusions and the Helmholtz oscillator consisting of one spring connected to a mass at one end and fixed at the other end

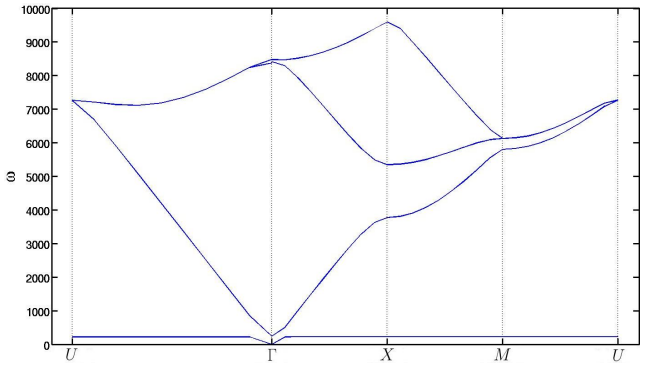

FIG. 4: Dispersion diagram for a periodic array (pitch $d=1$m) of spherical rigid shells (inner radius 0.3m and outer radius 0.4m) with one thin channel (length 0.1m and radius 0.01m) representing the frequency ω (Hz) of pressure waves in water versus the wavenumber $|\mathbf{k}|$ (m^{-1}), projection of the Bloch vector $\mathbf{k}$ along the edges of ΓXMU. We note the appearance of a frequency stop band for $\omega \in [224, 241]$Hz.

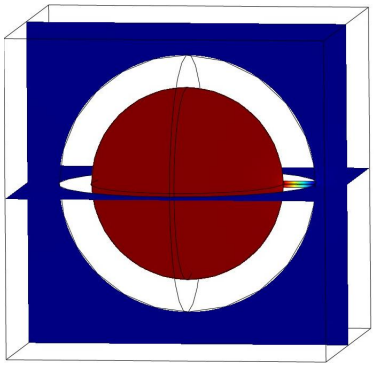

FIG. 5: The eigenfunction corresponding to the eigenfrequency $\omega_1^* = 224.6155$Hz for one thin channel. Blue color corresponds to nearly vanishing amplitude of the eigenmode u, while red color corresponds to it maximum value. The pressure field u is constant inside the inner cavity and outside the shell, but it varies rapidly inside the thin channel: it is a localised eigenmode responsible for the stop band in figure 4, which is well approximated by a spring mass model.

B. Eigenfrequency estimate in the case of a double spherical shell with one thin channel

In the numerical example we now have $\varepsilon^2 h_2^2 = 3.14.10^{-4}\text{m}^2$, $\varepsilon^2 h_1^2 = 7.85.10^{-5}\text{m}^2$, $l_2 = 0.1$m, $l_1 = 0.05$m, and the masses (in kilogram)

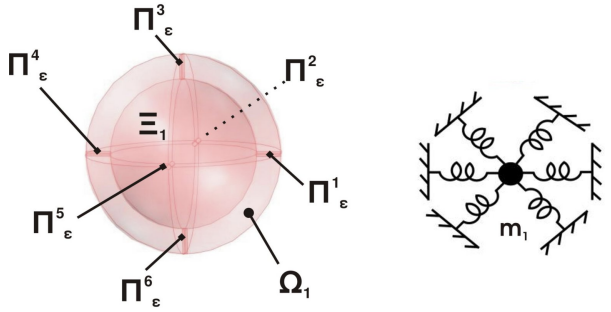

FIG. 6: Geometry of the inclusions and the Helmholtz oscillator consisting of six springs connected to a mass at one end and fixed at the other end

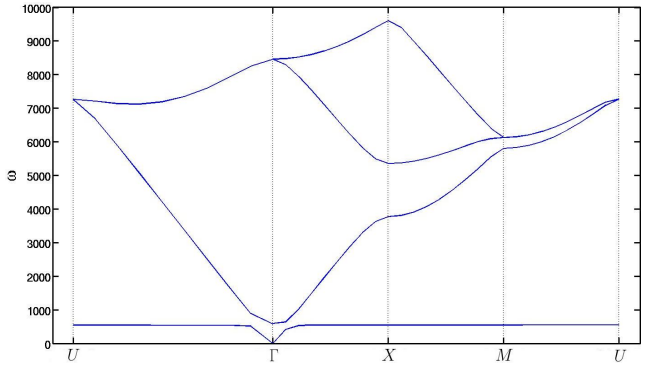

FIG. 7: Dispersion diagram for a periodic array (pitch $d = 1$m) of spherical rigid shells (inner radius $R = 0.3$m and outer radius $R = 0.4$m) with six thin channels (length 0.1m and radius 0.01m) representing the frequency ω (Hz) of pressure waves in water versus the wavenumber $|\mathbf{k}|$ (m^{-1}), projection of the Bloch vector $\mathbf{k}$ along the edges of ΓXMU. We note the appearance of a frequency stop band for $\omega \in [548, 588]$Hz which is wider and at higher frequencies than the stop band in figure 4: the more identical thin channels, the higher the resonant frequency of the localised mode.

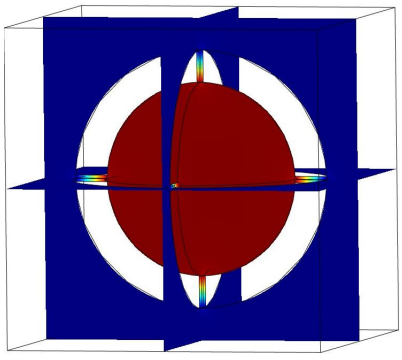

FIG. 8: The eigenfunction corresponding to the eigenfrequency $\omega_1^* = 548.3515$Hz for six thin channels responsible for the stop band in figure 7. This frequency is well approximate by the sping mass discrete model which provides us with the frequency estimate $\omega_1 = 556.772$Hz.

$$m_1 = \rho V_1 = \frac{4000}{3}\pi r_1^3$$
$$m_2 = \rho V_2 = \frac{4000}{3}\pi\left(r_1^3 + (b_2^3 - a_2^3)\right) + 10^3\varepsilon^2 h_1^2 l_1 \quad (26)$$

where ρ is the density of water ($\sim 10^3$kg.m^{-3}), V_1 and V_2 the volumes water occupies in Ξ_1 and Ξ_2, r_1 is the interior radius for the domain Ξ_1 and a_2, b_2 are respectively the interior and exterior radii for the domain Ξ_2. In our case, $r_1 = 0.1$m, $a_2 = 0.15$m and $b_2 = 0.2$m. The formula (21) gives the following values for the first eigenfrequencies (in Hertz) of the multistructures $\Pi_{\varepsilon(1)} \bigcup \Xi_{(1)}$ et $\Pi_{\varepsilon(2)} \bigcup \Xi_{(2)}$:

$$\omega_1 \sim 909.065 \quad , \quad \omega_2 \sim 542.026 \quad (27)$$

The corresponding frequencies (in Hertz) associated with the standing waves in the periodic structure were obtained numerically, and they are

$$\omega_1^* = 979.0268 \quad , \quad \omega_2^* = 470.286 \quad (28)$$

Formula (21) gives a good estimate for the eigenfrequency ω_1^*, but we observe a discrepancy in the approximation of ω_2^*. The estimate for the eigenfrequency ω_2^* can be improved if the domain $\Pi_{\varepsilon(2)} \bigcup \Xi_{(2)}$ is replaced by the domain $\Pi_{\varepsilon(2)} \bigcup \Omega_{(2)} \bigcup \Pi_{\varepsilon(1)} \bigcup \Omega_{(1)}$. In this case, the eigenfrequency ω_2 is approximated by the first positive eigenvalue of the problem

$$\rho^{-1} V_1''(x) + \lambda^{-1}\omega^2 V_1(x) = 0\,, \quad 0 < x < l_1 \quad (29)$$

$$V_1(0) = 0\,, \quad (30)$$

$$\lambda^{-1} I_1 V_1'(l_1) - \lambda^{-1} I_2 V_2'(0) = m_1\omega^2 V_1(l_1)\,, \quad (31)$$

$$\rho^{-1} V_2''(x) + \lambda^{-1}\omega^2 V_2(x) = 0\,, \quad 0 < x < l_2 \quad (32)$$

$$\lambda^{-1} I_2 V_2'(l_2) = m_2\omega^2 V_2(l_2)\,, \quad (33)$$

$$V_2(0) = V_1(l_1)\,, \quad (34)$$

where $V_1(x)$, $V_2(x)$ are the eigenfunctions defined on $(0, l_1)$ and $(0, l_2)$, respectively, and the masses m_1, m_2 are defined by (in kilogram)

$$m_1 = \frac{4000}{3}\pi r_1^3$$
$$m_2 = \frac{4000}{3}\pi\left(b_2^3 - a_2^3\right) \quad (35)$$

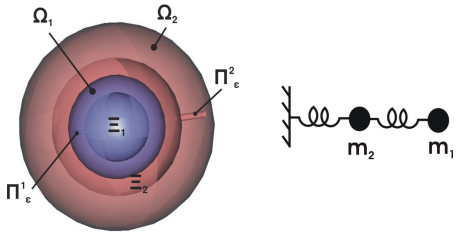

FIG. 9: Geometry of the inclusions and the Helmholtz oscillator consisting of two masses connected by a spring and one connected to a fixed domain.

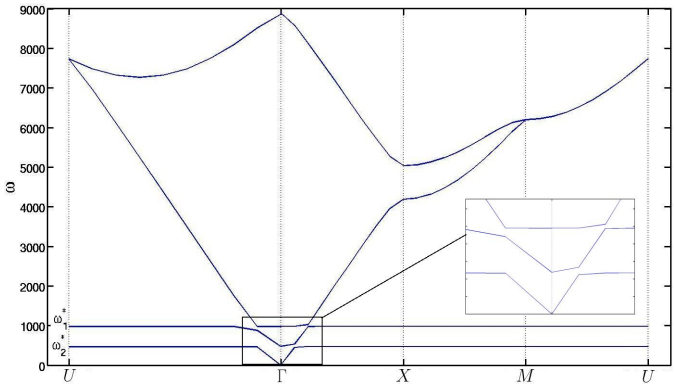

FIG. 10: Dispersion diagram for a periodic array (pitch $d = 1$m) of double spherical rigid shells (radius of spheres from inner to outer are 0.1m, 0.15m, 0.3m and 0.4m) with one thin channel in each shell (respectively of lengths 0.05m and 0.1m and radii 0.005m and 0.01m) representing the frequency ω (Hz) of pressure waves in water versus the wavenumber $|\mathbf{k}|$ (m^{-1}), projection of the Bloch vector $\mathbf{k}$ along the edges of ΓXMU. We note the appearance of two frequency stop bands for $\omega \in [470.2860, 476.5000]$Hz and $\omega \in [979.0268, 979.3559]$Hz.

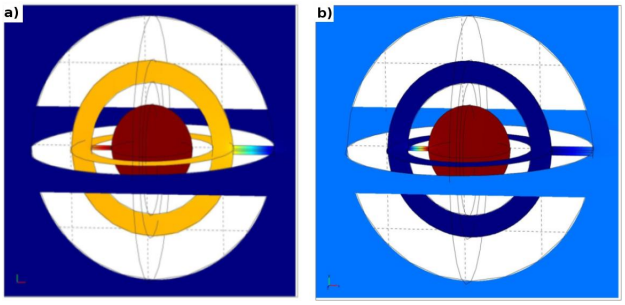

FIG. 11: a) The eigenfunction corresponding to the eigenfrequency $\omega_1^* = 979.0268$Hz. b) The eigenfunction corresponding to the eigenfrequency $\omega_2^* = 470.286$Hz. In (a) both canals vibrates, while in (b) only the inner canal does. Both frequencies are reasonably well approximated by the spring mass model which gives $\omega_1 = 909.065$Hz and $\omega_2 = 542.026$Hz.

Taking into account that $\omega_2 = O(\varepsilon)$, we deduce that it can be approximated as the first positive solution of the following algebraic equation:

$$m_1 m_2 l_1 l_2 \omega^4 - \lambda\omega^2 \left(l_2 I_1 m_1 + I_1 l_2 m_2 + I_2 m_1 l_1\right) + \lambda^2 I_1 I_2 = 0 \quad (36)$$

so that $\omega_2 \sim 520.121$Hz, which provides a more accurate approximation of $\omega_2^* = 470.286$H.

V. CONCLUSION

In this paper, we have seen that it is possible to sculpt the Bloch spectrum of three-dimensional phononic crystals ad libitum simply by digging some holes and adding cavities in rigid spheres periodically arranged along a cubic lattice. One of the main achievements of the numerical study is the appearance of ultra-low frequency stop bands at frequencies predicted quantitalively by an asymptotic model. We also conducted sozme basic shape optimization (by varying the size, diameter and number of channels in a rigid sphere of constant radius) in order to enhance the control of the location and the number of low frequency stop bands, thanks to our asymptotic estimates. Importantly, a cubic array of rigid spheres does not support any complete stop band, even in the densely packed configuration. Our findings are thus twofold: Multistructures open not only an original route toward ultra-low frequency stop bands (associated with very flat dispersion curves i.e. localized eigenmodes) but also offer the first paradigm of a complete stop band for three-dimensional pressure waves in a fluid. Finally, we illustrate in figure 12 a possible application of the ultra-low frequency stop band in order to localize a mode of a wavelength much larger than the pitch of the array of resonators. Similarly, one could envisage to reflect, detour, or focus, pressure waves using the low frequency stop band within which effective parameters are expected to take negative values as it is now well-established for the two-dimensional counterpart of such kind of acoustic metamaterials.

[1] J.P. Dowling, Photonic and Sonic Band Gap Metamaterial Bibliography: http://phys.lsu.edu/∼jdowling/pbgbib.html
[2] M. Kafesaki and E.N. Economou, Multiple-scattering theory for three-dimensional periodic acoustic composites, *Phys. Rev. B* **60**(17), 11993, 1999
[3] A.B. Movchan, N.V. Movchan and C.G. Poulton, Asymptotic models of fields in dilute and densely packed com-

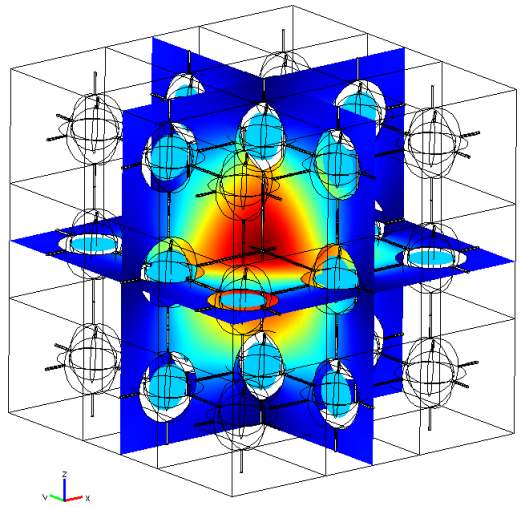

FIG. 12: The eigenfunction corresponding to the eigenfrequency $\omega_1^* = 224.6155$Hz for a macrocell of 26 resonators as in figures 4 and 5 with a defect (fluid instead of resonator) in the middle. The localised mode sits within the ultra-low frequency stop band of figure 4.

posites, Imperial College Press, 2002

[4] Z.Y. Liu, X.X. Zhang, Y.W. Mao, Y.Y. Zhu, Z.Y. Yang, C.T. Chan and P. Sheng, Locally resonant sonic materials, *Science* **289**, 1734, 2000

[5] J. Mei, Z. Liu, W. Wen and P. Sheng, Effective Mass Density of Fluid-Solid Composite, *Phys. Rev. Lett.* **96**, 024301, 2006

[6] V.A. Kozlov, V.G. Mazya and A.B. Movchan, Asymptotic analysis of fields in multi-structures, Oxford Research Monographs, Oxford University Press, 1999

[7] A.B. Movchan and S. Guenneau, *Phys. Rev. B* **70**, 125116, 2004

[8] S. Guenneau, A.B. Movchan, G. Petursson and S.A. Ramakrishna, Acoustic meta-materials for sound focussing and confinement, *New J. Phys.* **9**, 399, 2007

[9] J.B. Pendry, A.J. Holden, D.J. Robbins and W.J. Stewart, IEEE Trans. Microwave Theory Tech. **47**, 2075, 1999

[10] S. Guenneau, A.B. Movchan and N.V. Movchan, Localized bending modes in split ring resonators, *Physica B* **394**, 141 ,2007

[11] G.W. Milton, M. Briane and J.R. Willis, *New J. Phys.* **8**, 248, 2006

[12] M. Brun, S. Guenneau and A.B. Movchan, Achieving control of in-plane elastic waves, *Appl. Phys. Lett.***94**, 061903, 2009

[13] A. N. Norris Acoustic cloaking theory, *Proc. R. Soc. A***464**, 2411-2434, 2008

[14] A. N. Norris, Acoustic metafluids, *J. Acoust. Soc. Am.***125**, 839-849, 2009

[15] J. Li and C.T. Chan, Double negative acoustic metamaterial, *Phys. Rev. E* **70**, 055602, 2004

[16] N. Fang, D. Xi, J. Xu, M. Ambati, W. Srituravanich, C. Sun and X. Zhang, Ultrasonic metamaterials with negative modulus, *Nature* **5**, 452, 2006

[17] M. Farhat, S. Guenneau, S. Enoch and A.B. Movchan, Negative refraction, surface modes, and superlensing effect via homogenization near resonances for a finite array of split-ring resonators, *Phys. Rev. E* **80**, 046309, 2009

[18] F. Lemoult, M. Fink, and G. Lerosey, Acoustic Resonators for Far-Field Control of Sound on a Subwavelength Scale *Phys. Rev. Lett.***107**, 064301, 2011

[19] A. Nicolet, S. Guenneau, C. Geuzaine and F. Zolla, Modeling of electromagnetic waves in periodic media with finite elements, *J. Comp. Appl. Math.***168**, 321-329, 2004

[20] A.B. Movchan, N.V. Movchan and S. Haq, Localised vibration modes and stop bands for continuous and discrete periodic structures, *Materials Science Engineering A***431**, 175-183, 2006

[21] D. Bigoni, S. Guenneau, A.B. Movchan and M. Brun, Elastic metamaterials with inertial locally resonant structures : application to lensing, high-directivity and localisation, *Phys. Rev. B***87**(17), 174303, 2013

[22] R.V. Craster and S. Guenneau (Editors), Acoustic metamaterials : Negative refraction, imaging, lensing and cloaking, Springer Series in Materials Science **166**, 2013

[23] G. Stefan Llewellyn Smith and A.M.J. Davis, The split ring resonator, *Proc. R. Soc. A* **466**, 3117-3134, 2010